

Published in final edited form as:

Br J Ophthalmol. 2013 August ; 97(8): 1068–1073. doi:10.1136/bjophthalmol-2012-302881.

Lithium treatment increases endothelial cell survival and autophagy in a mouse model of Fuchs endothelial corneal dystrophy

Eun Chul Kim^{1,2}, Huan Meng¹, and Albert S Jun¹

¹ Cornea and Anterior Segment Division, Wilmer Eye Institute, Johns Hopkins Medical Institutions, Baltimore, Maryland, USA

² Department of Ophthalmology & Visual Science, College of Medicine, Catholic University of Korea, Seoul, Korea

Abstract

Background—Lithium previously has been shown to reduce both endoplasmic reticulum (ER) and oxidative stress in other in vitro and in vivo model systems. We investigated lithium's effects on cultured corneal endothelial cells (CECs) exposed to these types of stress and in a mouse model of Fuchs endothelial corneal dystrophy (FECD).

Methods—Viability of cultured bovine CECs was determined by CellTiter-Glo. 2-month-old *Col8a2*^{Q455K/Q455K} mutant (Q455K) and C57/Bl6 wild type animals were divided into two groups of 15 mice. Group I received 0.2% lithium carbonate-containing chow and Group II received control chow for 7 months. Confocal microscopy, transmission electron microscopy, real-time PCR (RT-PCR) and western blot were performed.

Results—Pretreatment with lithium increased viability of cultured CECs after H₂O₂ and thapsigargin exposure compared with untreated controls (p<0.05). In vivo analysis of mouse corneal endothelium showed the following: endothelial cell density of lithium treated Q455K was higher than for untreated Q455K (p<0.01). transmission electron microscopy of lithium treated Q455K showed normal endothelium with enlarged autophagosomes, but untreated Q455K showed dilated ER and guttae. Compared with untreated Q455K endothelium, lithium treated Q455K showed significant upregulation of *P62*, *Tmem74*, *Tm9sf1* and *Tmem 166* by RT-PCR and of *Atg5-12* conjugate by western blotting indicating that lithium treatment increased autophagy. Although RT-PCR unexpectedly showed increased levels of lithium response genes, caspase 12, *Gsk3*, *Arr 2* and *Impa1*, western blotting showed the expected downregulation of *Arr 2* and *Impa1* proteins in response to lithium treatment.

Conclusions—Lithium increases cultured CEC survival against ER and oxidative stress. Increased autophagy in lithium treated endothelium in a mouse model of FECD suggests autophagy may contribute to increased endothelial cell survival.

Correspondence to Dr Albert S Jun, Cornea and Anterior Segment Division, Wilmer Eye Institute, Johns Hopkins Medical Institutions, 400 N. Broadway, Smith 5011, Baltimore, MD 21231, USA; aljun@jhmi.edu.

Contributors All authors were involved in study design; data collection; data management and analysis; and data interpretation, preparation of the initial draft of manuscript, review and final approval of the manuscript. AJ takes overall responsibility for this work.

Competing interests None.

Provenance and peer review Not commissioned; externally peer reviewed.

Ethics approval Institutional Animal Care and Use Committee of Johns Hopkins University.

Data sharing statement Data available on request from the corresponding author Associate Prof. Albert S Jun.

INTRODUCTION

Fuchs endothelial corneal dystrophy (FECD) is characterised by progressive loss of corneal endothelial cells, alterations in the extracellular matrix and loss of vision from corneal clouding.¹ FECD affects upwards of 4% of the US population over the age of 40.² Currently no definitive non-surgical treatments exist for FECD, and this disorder is a leading cause of corneal transplantation accounting for upwards of 23% of cases.³ Mutations in multiple genes have been associated with FECD (for a complete list see <http://www.ncbi.nlm.nih.gov/omim/136800>) including a missense mutation resulting in a glutamine to lysine substitution at amino acid 455 (Q455K) in the $\alpha 2$ collagen VIII (*COL8A2*) gene causing an early onset form of the disease⁴ and a more common non-coding single nucleotide polymorphism in the transcription factor 4 (*TCF4*) gene linked to late onset disease.² Endoplasmic reticulum (ER) stress as shown by our previous work⁵ and oxidative stress as shown by others⁶ play important roles in the cellular pathogenesis of FECD. We have described previously a Q455K *Col8a2* transgenic knock-in mouse model of FECD which showed clinical features strikingly similar to human patients and also demonstrated endothelial cell ER stress and apoptosis, thereby confirming the role of ER stress in both early and late onset FECD.^{5,7}

Lithium has a wide range of protective cellular effects against a variety of stressors.⁸ Lithium reduces ER stress-mediated apoptosis via inhibition of caspase-12 and cleavage of caspase-3 in the ER.⁹ Lithium treatment can decrease the superoxide dismutase to catalase ratio significantly, which is associated with decreased oxidative stress by lowering hydrogen peroxide levels.⁸ Prolonged lithium pretreatment is cytoprotective against thapsigargin-induced cytotoxicity resulting from ER stress in PC12 cells.¹⁰ Lithium induces autophagy by way of the PI3K signalling pathway and has been proposed as a treatment for neurodegenerative diseases such as Huntington's disease.¹¹ Lithium overcomes the autophagic defect in CbCln3(ex7/8/ ex7/8) cerebellar cells and increases their viability under conditions of IMPase inhibition.¹² Given the protective effects of lithium against ER and oxidative stress, we sought to investigate its effects on cultured corneal endothelial cells exposed to these types of stress and on in vivo corneal endothelium in a mouse model of FECD.

METHODS

Cell culture

Bovine corneal endothelial cells were scraped from the excised corneas of freshly enucleated globes with a surgical blade, and primary cultures were established by resuspending cells in Dulbecco's modification of Eagle's minimum essential medium (Cellgro, Manassas, Virginia, USA) supplemented with 10% fetal calf serum, antibiotic antimycotic solution (10 000 units of penicillin (base), 10 000 μ g of streptomycin (base) and 25 μ g of amphotericin B/mL) (Invitrogen, Grand Island, New York, USA) and 50 μ g/mL of gentamicin (Invitrogen). Cells were grown at 37°C in 5% CO₂ in air on a 6-well plate (Cytoone, Orlando, Florida, USA). Once confluence was reached (usually 7–10 days), the primary cultures were subcultured to 96-well plates (Cytoone) in the same medium.

Cell treatment with lithium

Lithium carbonate (Sigma, St Louis, Missouri, USA) was freshly dissolved in phosphate-buffered saline (Gibco-BRL, Carlsbad, California, USA) at room temperature before use. To examine the effects of lithium on corneal endothelial survival, corneal endothelial cells were incubated in quadruplicate wells of a 96-well plate at several lithium concentrations (0–1000 μ M) for 48 h. After pretreatment with lithium for 48 h, the cultures were then treated with

100 μ L medium containing thapsigargin (28 μ M) for 24 h or H₂O₂ (0.6 mM) for 2 h at 37°C in a humidified 5% CO₂ atmosphere. Negative control (no lithium treatment and no H₂O₂ or thapsigargin conditioning) was also included to determine baseline cell viability. At the end of incubation, cell viability was determined by adding 100 μ L of CellTiter-Glo luminescent reagent (Promega, Madison, Wisconsin, USA) which produces light in direct proportion to the amount of ATP and viable cells present. The luminescence was measured using a FLUO star OPTIMA spectrophotometer (Optima, Tokyo, Japan). The cell viability (%) related to control was calculated by 100 \times luminescence in H₂O₂ or thapsigargin conditioned cells/ luminescence in the negative control (no lithium and no H₂O₂ or thapsigargin).

Animals

Weaned 2-month-old mice homozygous for the *Col8a2* Q455K mutation⁷ and 2-month-old wild type (WT) C57/Bl6 mice (Jackson Laboratory, Bar Harbor, Maine, USA) were divided into two groups of 30 mice for each treatment. Corneal endothelium from mutant mice at 2 months of age shows no differences with WT mice on confocal microscopy (unpublished data). Group I (lithium group, 15 mutant and 15 WT for a total of 30 mice) received 0.2% (weight/weight) lithium carbonate-containing chow (Harlan Teklad, <http://www.teklad.com>) and pure drinking water for 7 months. Group II (control group, 15 mutant and 15 WT for a total of 30 mice) received control rodent chow and pure drinking water for 7 months. All mice were housed in the Johns Hopkins Oncology Resources Animal Facility in accordance with guidelines of the Association for Assessment and Accreditation of Laboratory Animal Care International. The study protocols described herein were reviewed and approved by the Institutional Animal Care and Use Committee of Johns Hopkins University.

Confocal microscopy

All mice were euthanised by isoflurane (Vedco Inc., St Joseph, Missouri, USA), which was verified by checking for the absence of respirations followed by cervical dislocation. Immediately after euthanasia, one eye of each mouse was randomly selected for examination by confocal microscopy (Nidek Confoscan 3, Fremont, California, USA). Endothelial cell imaging and quantitative analyses were performed using the Confoscan 3 software.

Transmission electron microscopy

Both eyes of two mice (four eyes total) randomly selected from each group were analysed. After confocal microscopic examination, whole globes were enucleated and fixed in 2.5% glutaraldehyde/2% paraformaldehyde, pH 7.4, overnight at 48°C. Corneas were excised and bisected. Corneal halves were then washed in 0.1 M phosphate buffer followed by a 2 h, room temperature fixation in 1% osmium tetroxide in 0.1M phosphate buffer, pH 7.4. The specimens were then washed and dehydrated in a series of 50%–100% ethanol followed by a 1 h fixation in 1% uranyl acetate in 100% ethanol at room temperature in the dark. Postdehydration, specimens were washed twice in propylene oxide for 15 min each and incubated in a 1:1 mixture of propylene oxide to LX-112 resin (Ladd Research, Williston, Vermont, USA) overnight at room temperature. Specimens were submerged in 100% resin, subjected to vacuum for 5 h before embedding in freshly made LX-112 resin, and polymerised at 60°C for 2 days before sectioning. A total of 68 nanometer ultrathin sections were cut with a Leica Ultramicrotome UCT (Wetzlar, Germany) and imaged using a Hitachi H7600 transmission electron microscope (Pleasanton, California, USA).

Real-time PCR

After confocal microscopic examination, a total of five mice were randomly selected from each group. Both eyes of each mouse were extracted, Descemet membranes (DMs) were stripped with forceps, and both DMs containing endothelium from a single mouse were

pooled as a single sample (n). Five mice (n=5) were used for each group. Total RNA was extracted from murine corneal endothelium using TRIzol reagent (Invitrogen) followed by RNeasy column (Qiagen, Hilden, Germany) purification. Complementary DNA was generated using the High Capacity cDNA Reverse Transcription Kit (Applied Biosystems, Foster City, California, USA). The resulting complementary DNA (3 μ L cDNA) was preamplified with TaqMan PreAmp MasterMix and mouse specific primers (PCR primers for the examined genes are listed in table 1). RT-PCR was performed using the TaqMan Gene Expression Master Mix (2 \times) (Applied Biosystems), preamplified cDNA products (diluted 1:20; 5 μ L), nuclease free water and mouse specific primers in a 20 μ L reaction volume. The relative gene expression in Col8a2^{Q455K/Q455K} and WT endothelium was normalised to β -actin. A no-template control was included in each quantitative RT-PCR experiment to confirm the absence of DNA contamination. All assays used similar amplification efficiency, and a C_T experimental design was used for relative quantification. Data analysis was performed using StepOne software (V.2.2, Applied Biosystems). Statistical analysis of quantitative RT-PCR data between the groups was performed using analysis of variance (ANOVA) and DataAssist Software V.3.0 (Applied Biosystems). A p value<0.05 was considered statistically significant.

Western blotting

After confocal microscopic examination, a total of four mice were randomly selected from each group. Both eyes of each mouse were extracted, DMs were stripped with forceps and both DMs containing endothelium from a single mouse were pooled as a single sample (n). Four mice (n=4) were used for each group. DM and endothelial cells were homogenised in Tissue Protein Extract Reagent (Thermo Fisher Scientific, Rockford, Illinois, USA) with 1% protease inhibitor cocktail (Sigma) and 1% ethylenediaminetetraacetic acid (Sigma). The mixture was then microcentrifuged for 10 min at 12 000 rpm. The lysate was removed and the protein concentration was quantified by BCA Protein Assay Kit (Thermo Fisher Scientific). An amount of 8 μ g of protein were mixed with 10 μ L of 4 \times loading dye (NuPage, Invitrogen, Carlsbad, California, USA) with 2-mercaptoethanol (Sigma) and heated at 65°C for 5 min.

Samples were loaded onto a 10% Tris-HCl Ready Gel (BioRad, Hercules, California, USA) and subjected to sodium dodecylsulfate-polyacrylamide gel electrophoresis separation for 1 h at 120 V. Proteins were transferred to a polyvinylidene fluoride membrane (BioRad) and incubated in blocking buffer made of 5% non-fat milk in phosphate-buffered saline with 0.1% Tween-20. Membranes were then incubated in primary antibodies: *Atg5-12* conjugate (1: 500, Cell Signaling Technology, Beverly, Massachusetts, USA), inositol monophosphatase 1 (*Impa1*) (1: 500, Cell Signaling Technology) and *Arr 2* (1: 500, Cell Signaling Technology) diluted in blocking buffer for 1 h at room temperature. Subsequently, membranes were washed and incubated in 1:10 000 dilution of antirabbit IgG, horseradish peroxidase conjugated antibody (GE Healthcare, Piscataway, New Jersey, USA) diluted in blocking buffer for 45 min at room temperature. Loading controls were assayed by probing with β -actin (1:1000, Cell Signaling Technology) as primary antibody after stripping with Restore Stripping Buffer (Thermo Fisher Scientific). Low abundance proteins were detected using SuperSignal West Dura (Thermo Fisher Scientific) and higher abundance proteins were detected using HyGlo Quick Spray (Denville Scientific, Metuchen, New Jersey, USA). Densitometry analysis was performed using Image J as previously described (<http://www.lukemiller.org/journal/2007/08/quantifying-western-blots-without.html>).

Statistics

Data are presented as mean \pm SD. Significance of cell viability according to lithium concentration and cell density (CD) and hexagonality by confocal microscopy was

determined by one-way ANOVA using a two-tailed test. In scatter-plot graphs, symbols denote individual mice or assays, and horizontal bars represent means. RT-PCR and western blot assay results were compared using the two-tailed Student t test. A p value less than 0.05 was considered significant.

RESULTS

Cell culture

We initially evaluated the survival effects of lithium on cultured bovine corneal endothelial cells exposed to ER stress (thapsigargin 28 μM) and oxidative stress (H_2O_2 0.6 mM). Bovine cells were used initially instead of mouse cells due to the practical difficulties involved in culturing mouse endothelium. Viability of H_2O_2 exposed cells pretreated with 300 μM ($62.2\% \pm 3.50\%$) and 1000 μM ($67.7\% \pm 2.8\%$) lithium was significantly increased compared with untreated controls ($57.5\% \pm 2.5\%$) (figure 1A). Viability of thapsigargin exposed cells pretreated with 300 μM ($59.9\% \pm 3.0\%$) and 1000 μM ($65.0\% \pm 3.9\%$) lithium was significantly increased compared with untreated controls ($56.0\% \pm 2.1\%$) (figure 1A).

Confocal microscopy

Endothelium of lithium treated Q455K mice showed a mild phenotype with few extracellular matrix excrescences (guttae) (white arrows, figure 1B), and mild variation in cell size and shape. In contrast, endothelium from untreated, control Q455K mice showed a more severe phenotype with multiple guttae and increased variation in cell size and shape. Endothelium from lithium treated and untreated WT mice showed a normal phenotype with no guttae and a characteristic monolayer of hexagonal cells with highly regular size and shape (figure 1B). Corneal endothelial CD of lithium treated Q455K mice (1847 ± 227 cells/ mm^2) was 25% higher than for untreated Q455K mice (1472 ± 85) ($p < 0.01$, figure 1C). CD of untreated, control WT mice (2207 ± 133 cells/ mm^2) was significantly higher than both lithium treated and untreated Q455K mice (figure 1C). Per cent hexagonal cells, an additional marker of CEC integrity, was 22% higher in lithium treated Q455K mice ($32.6\% \pm 7.6\%$) and 38% higher in untreated WT mice ($37.0\% \pm 9.4\%$) compared with untreated Q455K mice ($26.8\% \pm 8.25$) ($p < 0.01$ for both, figure 1C).

Transmission electron microscopy

Lithium treated Q455K corneal endothelium showed a combination of normal appearing cells with compact organelles (figure 2A) and cells with grossly enlarged autophagosomes containing remnants of degraded organelles (figure 2B). Untreated, control Q455K endothelium showed severely dilated ER filled with proteinaceous material (figure 2C) and guttae attached to the underlying basement membrane (DM) of the endothelium (figure 2D). Additional images of guttae (not shown) further indicate that these guttae attached to the basement membrane originate as portions of dead cells. Lithium treated and untreated WT controls showed normal endothelial cells (figure 2E–H).

RT-PCR and western blotting

To confirm activation of the unfolded protein response in Q455K mouse endothelium, we used RT-PCR to assay for expression of 78 kDa glucose regulated protein (*Grp 78*) and C/EBP homologous protein (*Chop*).¹³ These markers were significantly upregulated in lithium treated (*Grp78*: 1.74 ± 0.37 , *Chop*: 1.38 ± 0.21 -fold) and untreated (*Grp78*: 1.67 ± 0.19 , *Chop*: 1.35 ± 0.18 -fold) Q455K mice compared with untreated WT mice (figure 3A). Given the presence of enlarged autophagosomes in the endothelium of lithium treated Q455K (Q455K-Lithium) mice, we sought to evaluate for the following markers of autophagy in Q455K-Lithium and untreated Q455K (Q455K-Control) endothelium. Q455K-Lithium endothelium

showed significant upregulation of autophagy markers *P62* (2.15±0.10-fold), *Tmem74* (4.80±1.99-fold), *Tm9sf1* (1.48 ±0.14-fold), and *Tmem166*¹⁴ (2.70±0.57-fold) by RT-PCR and of *Atg5-12* conjugate¹⁵ (1.29±0.06-fold) by western blotting compared with Q455K-Control endothelium (figure 3B). Finally, we sought to confirm cellular effects of lithium by assaying expression of the following genes associated with downregulation by lithium treatment. Surprisingly, significant upregulation of *Caspase 12* (1.65±0.02-fold), *Gsk3* (1.52±0.21-fold), *Arr 2* (1.61±0.17-fold) and *Impa1* (1.35±0.18-fold) were found by RT-PCR in Q455K-Lithium versus untreated Q455K-Control endothelium (figure 3C). However, western blotting showed the expected downregulation of *Impa1* (0.68±0.14-fold) and *Arr 2* (0.41±0.22-fold) in Q455K-Lithium versus untreated Q455K-Control endothelium (figure 3C).

DISCUSSION

FECD is characterised by progressive loss of corneal endothelial cells and is a leading cause of corneal transplant surgery.¹ ER and oxidative stress contribute to the pathogenesis of FECD.⁵⁶ Lithium prevents ER and oxidative stress-mediated apoptosis via a variety of cellular effects,¹⁶ and we found that lithium increases survival in cultured corneal endothelial cells exposed to ER and oxidative stress. Although highly reproducible, the relatively modest increase in survival in lithium treated versus untreated cultured cells may reflect the higher intensity and shorter duration cell stress used in the culture system compared with presumably lower levels and longer duration cell stress in vivo.

Given others' work and our initial results in cultured corneal endothelial cells indicating the protective effects of lithium against ER and oxidative stress, we sought to evaluate the effects of chronic, oral, low-dose lithium treatment on the corneal endothelium in vivo using our knock-in mouse model of FECD homozygous for the Q455K *Col8a2* mutation. In clinical confocal images of 9-month-old animals, endothelium of lithium treated Q455K mice showed mild endothelial guttae highly characteristic of FECD, but endothelium from untreated Q455K mice showed multiple guttae and increased variation in cell size and shape. Corneal endothelial CD and per cent hexagonal cells of lithium treated Q455K mice were higher than for untreated Q455K mice. Thus, chronic oral administration of lithium in a transgenic knock-in mouse model of FECD results in increased endothelial cell survival.

Based on the positive in vivo effects of lithium on endothelial CD and morphology, we performed transmission electron microscopy to evaluate its effects on the ultrastructure of corneal endothelial cells. Lithium treated Q455K corneal endothelium showed normal appearing cells interspersed with cells containing grossly enlarged autophagosomes, whereas untreated Q455K endothelium showed severely dilated ER and guttae. We hypothesised that increased autophagy induced by lithium might enhance cell survival in Q455K endothelium exposed to ER stress. Thus, we next confirmed increased expression of autophagy markers in the endothelium of lithium treated Q455K mice compared with untreated control Q455K mice. Finally, we sought to confirm the pharmacological effects of lithium on the corneal endothelium of treated animals by assessing the expression of caspase 12,⁹ glycogen synthase kinase 3 (*Gsk3*), arrestin 2 (*Arr 2*) and *Impa1*.¹⁶ Somewhat surprisingly, lithium caused upregulation of caspase 12, *Gsk3*, *Arr 2* and *Impa1* by RT-PCR, whereas western blotting showed the expected downregulation of *Arr 2* and *Impa1*. Chronic lithium treatment has been shown to upregulate *Impa1* mRNA levels in mouse hippocampus which may reflect a compensatory response to inositol depletion.¹⁷ A similar phenomenon could explain the apparent inconsistency between mRNA and protein levels in our selected lithium response genes.

Induction of autophagy by lithium is neuroprotective and is associated with inhibition of IMPA.¹¹¹² Autophagy is a complex cellular process which occurs in response to ER stress and oxidative stress as a mechanism to enhance cell survival.¹⁸¹⁹ Given the role of ER stress in FECD,⁵⁷ it is provocative to suggest that the endothelial cell survival effect of lithium described here is primarily mediated through increased autophagy. However, other possibilities cannot be excluded such as lithium's antiapoptotic effects resulting from inhibition of glycogen synthase kinase 3.¹⁶

In conclusion, our results reveal that lithium can increase corneal endothelial survival in a cell culture and mouse model of FECD and thus represent the first in vivo evidence of a potential medical treatment for FECD. Our findings further suggest that increasing autophagy through other agents in addition to lithium may be a rational therapeutic approach. As mutations in multiple genes (*COL8A2*, *SLC4A11*, *TCF4*, *TCF8*, *LOXHD1* and *CLU/TGFB1*) have been associated with causing FECD,^{2, 4, 20, 24} additional work will be needed to confirm whether lithium and increased autophagy can improve the disease course associated with other genetic causes of FECD. As previous reports demonstrating the role of ER and oxidative stress in FECD used genetically undifferentiated (ie, unknown genotypes), late stage disease tissue obtained at corneal transplantation,⁵⁶ we speculate that lithium's cytoprotective effects against these processes could make it a generalised 'endothelial survival factor' with broad therapeutic effects in FECD. Future investigations of lithium as a treatment for FECD could involve clinical trials to assess its efficacy in patients with different genetic causes of FECD as well as to assess for adverse effects of treatment which are well documented with lithium's use in psychiatric disease. However, the use of topical or local routes of ocular administration, if technically feasible, could be attractive approaches to mitigate the latter issue.

Acknowledgments

Funding The authors' work is supported by grants from the National Institutes of Health (NIH EY019874 to ASJ and EY001765 to Wilmer Microscopy Core Facility), Medical Illness Counseling Center and the J Willard and Alice S Marriott Foundation (both to ASJ), and Research to Prevent Blindness (to Wilmer Eye Institute) and research funds generously provided by Lorraine Collins, Richard Dianich, Stanley Friedler, MD, Diane Kemker, Jean Mattison, Lee Silverman and Norman Tunkel.

REFERENCES

1. Elhalis H, Azizi B, Jurkunas UV. Fuchs endothelial corneal dystrophy. *Ocul Surf.* 2010; 8:173–84. [PubMed: 20964980]
2. Baratz KH, Tosakulwong N, Ryu E, et al. E2–2 protein and Fuchs's corneal dystrophy. *N Engl J Med.* 2010; 363:1016–24. [PubMed: 20825314]
3. Dobbins KR, Price FW Jr, Whitson WE. Trends in the indications for penetrating keratoplasty in the midwestern United States. *Cornea.* 2000; 19:813–16. [PubMed: 11095055]
4. Biswas S, Munier FL, Yardley J, et al. Missense mutations in *COL8A2*, the gene encoding the alpha2 chain of type VIII collagen, cause two forms of corneal endothelial dystrophy. *Hum Mol Genet.* 2001; 10:2415–23. [PubMed: 11689488]
5. Engler C, Kelliher C, Spitze AR, et al. Unfolded protein response in fuchs endothelial corneal dystrophy: a unifying pathogenic pathway? *Am J Ophthalmol.* 2010; 149:194–202. [PubMed: 20103053]
6. Azizi B, Ziaei A, Fuchsluger T, et al. p53-regulated increase in oxidative-stress– induced apoptosis in Fuchs endothelial corneal dystrophy: a native tissue model. *Invest Ophthalmol Vis Sci.* 2011; 52:9291–7. [PubMed: 22064994]
7. Jun AS, Meng H, Ramanan N, et al. An alpha 2 collagen VIII transgenic knock-in mouse model of Fuchs endothelial corneal dystrophy shows early endothelial cell unfolded protein response and apoptosis. *Hum Mol Genet.* 2012; 21:384–93. [PubMed: 22002996]

8. Khairova R, Pawar R, Salvatore G, et al. Effects of lithium on oxidative stress parameters in healthy subjects. *Mol Med Report*. 2012; 5:680–2.
9. Ghribi O, Herman MM, Savory J. Lithium inhibits Abeta-induced stress in endoplasmic reticulum of rabbit hippocampus but does not prevent oxidative damage and tau phosphorylation. *J Neurosci Res*. 2003; 71:853–62. [PubMed: 12605412]
10. Hiroi T, Wei H, Hough C, et al. Protracted lithium treatment protects against the ER stress elicited by thapsigargin in rat PC12 cells: roles of intracellular calcium, GRP78 and Bcl-2. *Pharmacogenomics J*. 2005; 5:102–11. [PubMed: 15668729]
11. Sarkar S, Floto RA, Berger Z, et al. Lithium induces autophagy by inhibiting inositol monophosphatase. *J Cell Biol*. 2005; 170:1101–11. [PubMed: 16186256]
12. Chang JW, Choi H, Cotman SL, et al. cerebellar cells and reduces neuronal vulnerability to cell death via IMPase inhibition. *J Neurochem*. 2011; 116:659–68. [PubMed: 21175620]
13. Malhi H, Kaufman RJ. Endoplasmic reticulum stress in liver disease. *Hepatology*. 2011; 54:795–809.
14. He P, Peng Z, Luo Y, et al. High-throughput functional screening for autophagy-related genes and identification of TM9SF1 as an autophagosome-inducing gene. *Autophagy*. 2009; 5:52–60. [PubMed: 19029833]
15. Yang YP, Liang ZQ, Gu ZL, et al. *Acta Pharmacol Sin*. 2005; 26:1421–34. [PubMed: 16297339]
16. Freland L, Beaulieu JM. Inhibition of GSK3 by lithium, from single molecules to signaling networks. *Front Mol Neurosci*. 2012; 5:14. [PubMed: 22363263]
17. Shamir A, Shaltiel G, Greenberg ML, et al. The effect of lithium on expression of genes for inositol biosynthetic enzymes in mouse hippocampus; a comparison with the yeast model. *Brain Res Mol Brain Res*. 2003; 115:104–10. [PubMed: 12877981]
18. Sheng R, Liu XQ, Zhang LS, et al. Autophagy regulates endoplasmic reticulum stress in ischemic preconditioning. *Autophagy*. 2012; 8:310–25. [PubMed: 22361585]
19. Lee J, Giordano S, Zhang J. Autophagy, mitochondria and oxidative stress: cross-talk and redox signalling. *Biochem J*. 2012; 441:523–40. [PubMed: 22187934]
20. Vithana EN, Morgan PE, Ramprasad V, et al. SLC4A11 mutations in Fuchs endothelial corneal dystrophy. *Hum Mol Genet*. 2008; 17:656–66. [PubMed: 18024964]
21. Thalamuthu A, Khor CC, Venkataraman D, et al. Association of TCF4 gene polymorphisms with Fuchs' corneal dystrophy in the Chinese. *Invest Ophthalmol Vis Sci*. 2011; 52:5573–8. [PubMed: 21659310]
22. Mehta JS, Vithana EN, Tan DT, et al. Analysis of the posterior polymorphous corneal dystrophy 3 gene, TCF8, in late-onset Fuchs endothelial corneal dystrophy. *Invest Ophthalmol Vis Sci*. 2008; 49:184–8. [PubMed: 18172091]
23. Riazuddin SA, Parker DS, McGlumphy EJ, et al. Mutations in LOXHD1, a recessive-deafness locus, cause dominant late-onset Fuchs corneal dystrophy. *Am J Hum Genet*. 2012; 90:533–9. [PubMed: 22341973]
24. Kuot A, Hewitt AW, Griggs K, et al. Association of TCF4 and CLU polymorphisms with Fuchs' endothelial dystrophy and implication of CLU and TGFBI proteins in the disease process. *Eur J Hum Genet*. 2012; 20:632–8. [PubMed: 22234156]

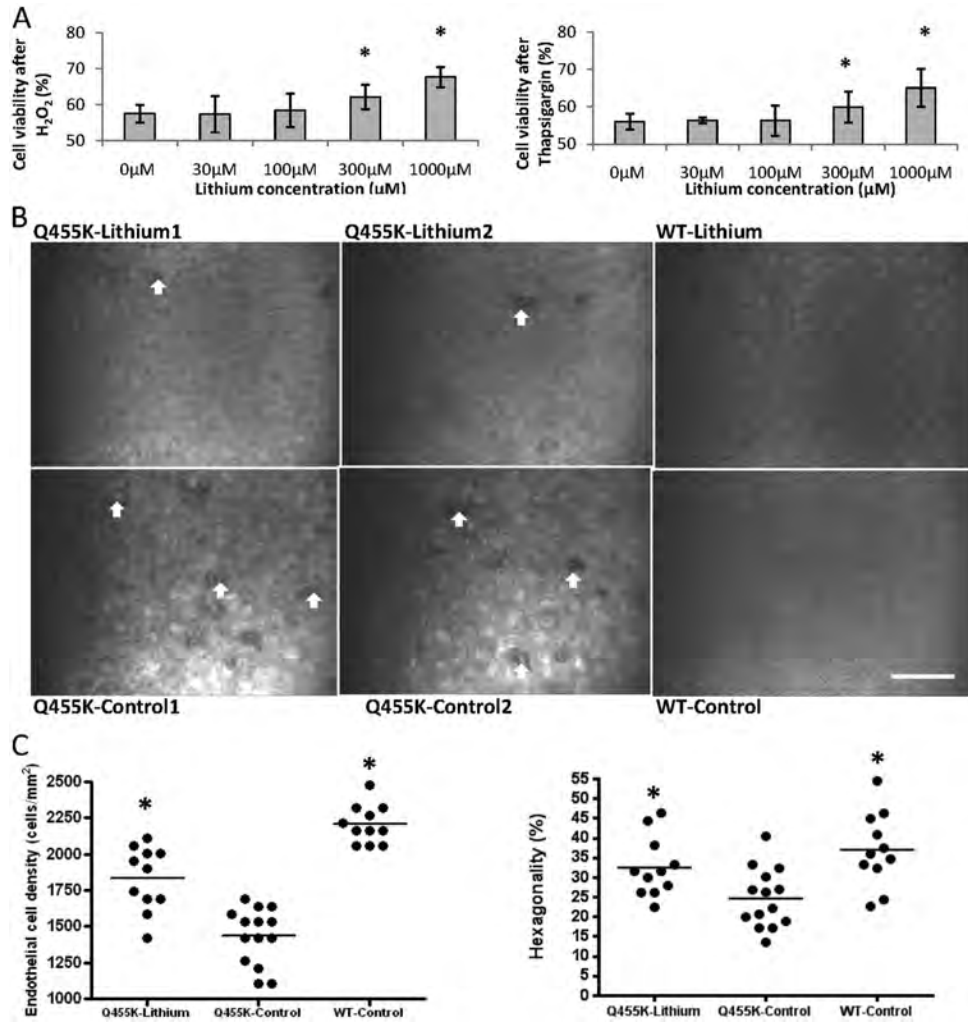


Figure 1. (A) Cell viability of lithium treated bovine corneal endothelial cells after H₂O₂ or thapsigargin conditioning increased compared with untreated control (*p<0.05). Data represent the mean±SD. (B) Confocal images of corneal endothelial cells in homozygous Q455K mutant mice treated with lithium (Q455K-Lithium, representative images from two animals shown) have fewer guttae (white arrows) and relatively normal cell size and shape compared with untreated homozygous Q455K (Q455K-Control, representative images from two animals shown) mice. Wild type mice treated (WT-Lithium) or untreated (WT-Control) with lithium show normal endothelium (scale bar=60 μM for all panels). (C) Scatter plot shows higher corneal endothelial cell density in Q455K-Lithium mice compared with untreated Q455K-Control mice. Untreated WT-Control mice are shown for comparison. Percent hexagonality of corneal endothelial cells in Q455K-Lithium mice is higher than Q455K-Control group (*p<0.01 compared with Q455K-Control). Horizontal bars=mean.

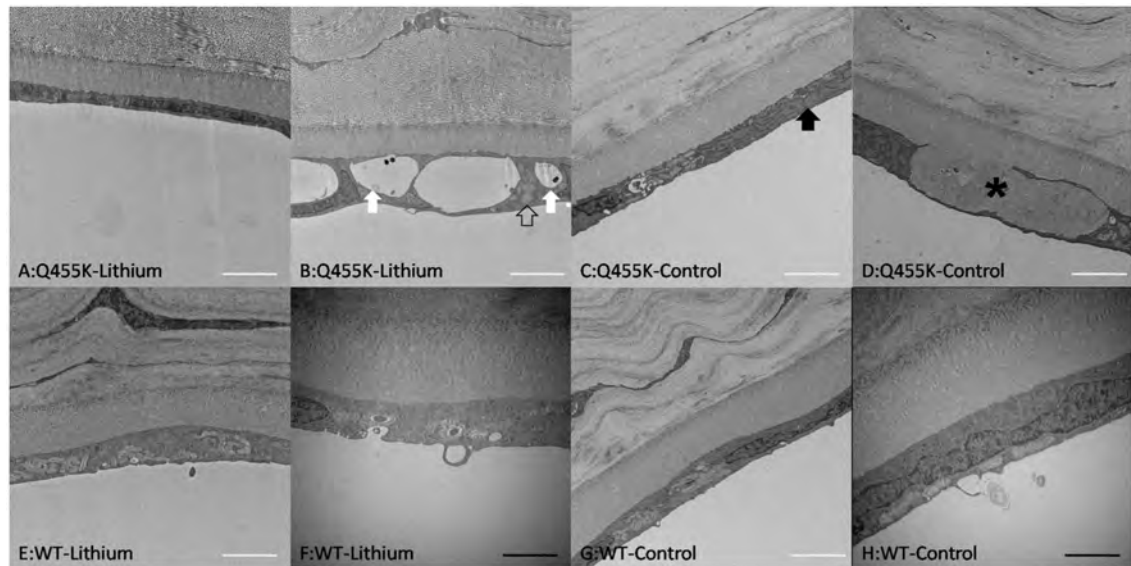


Figure 2.

Transmission electron microscopy of corneal endothelial cells in homozygous mutant Q455K mice treated with lithium (Q455K-Lithium) shows variation between normal appearance (A) and markedly enlarged autophagosomes containing intracellular remnants (B, white arrows) with normal mitochondria (B, empty arrow). Untreated control homozygous mutant Q455K mice (Q455K-Control) show (C) dilated rough endoplasmic reticulum (black arrow) and (D) basement membrane excrescences (guttae, *). Wild type mice treated (WT-Lithium, E and F) or untreated (WT-Control, G and H) with lithium show normal endothelium (white scale bar=2 μ m, black scale bar=500 nm).

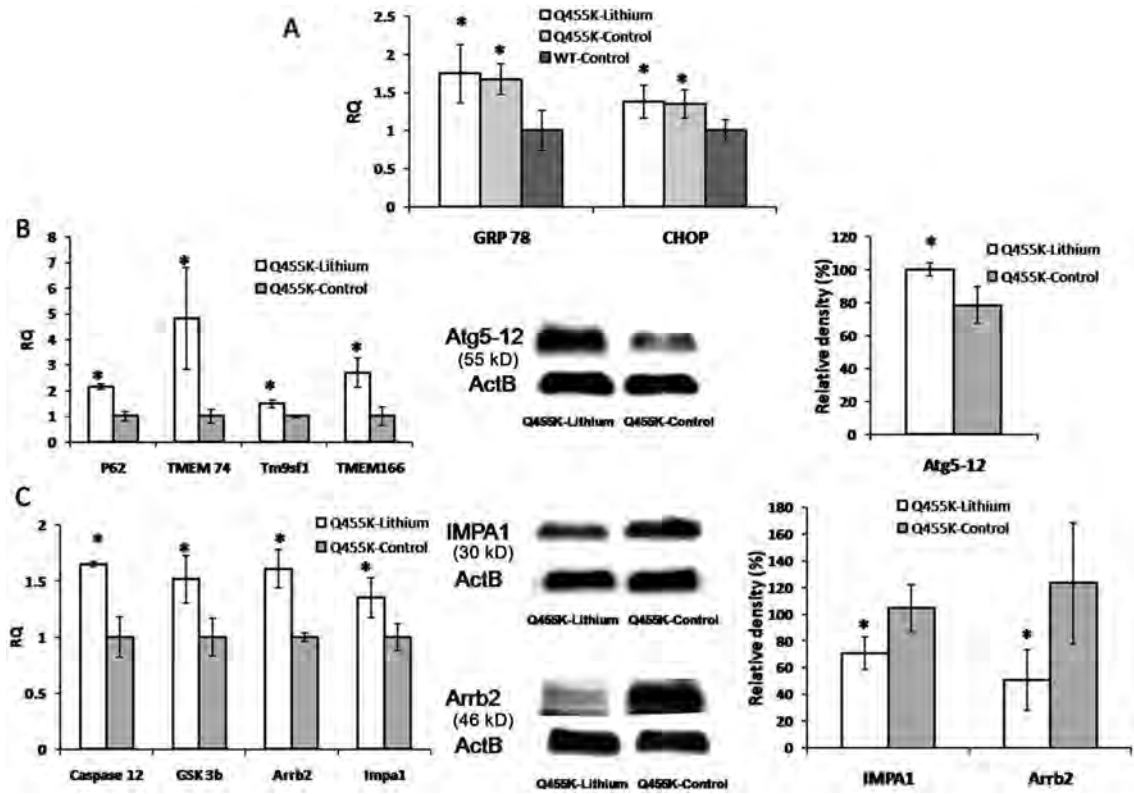


Figure 3.

(A) Real-time PCR (RT-PCR) shows upregulation of GRP 78 and CHOP in both Q455K-Lithium and Q455K-Control groups compared with untreated wild type-Control group (relative quantity (RQ)=1) (* $p < 0.05$). (B) RT-PCR shows upregulation of autophagy related genes (*P62*, *Tmem74*, *Tm9sf1* and *Tmem166*) in Q455K-Lithium versus untreated Q455K-Control (RQ=1). Western blot analysis with densitometry normalised to β -actin (ActB) shows increased levels of autophagy markers Atg5-12 in Q455K-Lithium group compared with Q455K-Control group (* $p < 0.05$). (C) RT-PCR for genes associated with downregulation by lithium treatment (*Caspase 12*, *GSK 3*, *Arr 2* and *Impa1*) showed upregulation, but western blot analysis showed decreased levels of *Impa1* and *Arr 2* in Q455K-Lithium group compared with Q455K-Control group (* $p < 0.05$).

Table 1

Primer sets used for real-time PCR analysis

Gene	Symbol	GenBank reference sequence	Assay number*
Heat shock protein 5	<i>Hspa5</i> (<i>Grp78</i>)	NM_001163434.1	Mm00517690_g1
DNA damage inducible transcript 3	<i>Ddit3</i> (<i>Chop</i>)	NM_007837.3	Mm01135937_g1
Caspase 12	<i>Casp12</i>	NM_009808.4	Mm00438038_m1
Glycogen synthase kinase 3	<i>Gsk3</i>	NM_019827.6	Mm00444911_m1
Arrestin, 2	<i>Arr 2</i>	NM_145429.4	Mm00520674_m1
Inositol monophosphatase 1	<i>Imp1</i>	NM_018864.5	Mm00497770_m1
Sequestosome 1	<i>Sqstm1</i> (<i>P62</i>)	NM_011018.2	Mm00448091_m1
Transmembrane protein 74	<i>Tmem74</i>	NM_175502.3	Mm01164476_m1
Transmembrane 9 superfamily member 1	<i>Tm9sf1</i>	NM_028780.3	Mm00446042_m1
Transmembrane protein 166	<i>Tmem166</i>	NM_008046	Mm00514982_m1
-Actin	<i>Actb</i>	NM_007393.3	Mm00607939_s1

* Applied Biosystems, Foster City, California, USA.